Numerical analysis of repetitive pulsed-discharge de-NO x process with ammonia injection

Kazuo Onda, Hironobu Kusunoki, Kohei Ito, and Hiroshi Ibaraki

Citation: Journal of Applied Physics **95**, 3928 (2004); doi: 10.1063/1.1682686
View online: http://dx.doi.org/10.1063/1.1682686
View Table of Contents: http://scitation.aip.org/content/aip/journal/jap/95/8?ver=pdfcov
Published by the AIP Publishing

Numerical analysis of repetitive pulsed-discharge de-NO_x process with ammonia injection

Kazuo Onda,[a] Hironobu Kusunoki, Kohei Ito, and Hiroshi Ibaraki
Department of Electric and Electronic Engineering, Toyohashi University of Technology, 1-1 Hibarigaoka, Tenpaku, Toyohashi, Aichi 441-8580, Japan

(Received 8 September 2003; accepted 20 January 2004)

Due to its relatively high-performance and compactness, the pulsed-discharge de-NO_x process is expected to be an advanced technology to suppress air pollution. Adequate guidelines for optimum operation of the pulsed-discharge de-NO_x process have not yet been established however. In this study, we numerically analyze the process subjected to several hundred high-voltage pulses and investigate the effects of by-products and ammonia injection on the de-NO_x performance. The electron collision process to produce OH and N radicals to remove NO_x is analyzed by the Boltzmann equation for the energy distribution of discharge electrons. The chemical reaction process between the unstable radicals and NO_x including combustion flue gas is calculated by considering a total of 1004 rate equations for electron collision and chemical reaction processes and a total of 101 chemical species. In a case without ammonia injection, both the N_xO_y removal efficiency and the de-NO_x energy consumption rate to remove N_xO_y change with an increase in repeated pulse number because electrons produced by the discharge attach to accumulated by-products, such as $H_3O^+(H_2O)_2$, followed by a decrease in radical concentration, i.e., a decrease in oxidative and reductive removal reaction rates. In the case with ammonia injection, the removal efficiency increases and the electric energy consumption rate decreases with an increase in ammonia concentration because removal reactions such as $NO \rightarrow NO_2 \rightarrow HNO_3 \rightarrow NH_4NO_3$ and $NO \rightarrow N_2$ are promoted. When excess ammonia is injected, the de-NO_x performance declines because the NH_2 radical produced by electron collision with ammonia reacts with NO_2 and forms relatively stable N_2O. In a case where HNO_2 is considered N_xO_y, the de-NO_x performance is also assessed.
 [DOI: 10.1063/1.1682686]

I. INTRODUCTION

Economically advantageous, high-performance exhaust gas processing technologies are being sought to prevent the spread of environmental pollution. The development of methods for efficiently removing nitrogen oxides (NO_x) produced in combustion processes is particularly desirable. One candidate for NO_x processing technology is denitrification through pulse discharge. In this method, it is known that nonequilibrium plasma is generated by application of a pulse voltage and it generates N and OH radicals through dissociation of combustion gas by collision of discharge electrons, and the radicals generated preferentially react with NO_x. This discharge process has been demonstrated experimentally to show good denitrification performance, and various kinds of discharge methods have been studied and developed to date. To implement this pulse discharge process in practical technology, it is necessary to properly understand the discharge de-NO_x process to estimate both the forming and quenching radical concentrations, and to optimize operating conditions such as the voltage applied and pulse width in order to obtain good quantitative de-NO_x performance. The superiority of this method over other de-NO_x methods must also be clarified.

[a]Electronic mail: onda@eee.tut.ac.jp

Up to this point, we have numerically analyzed the discharge de-NO_x process, and clarified the effects of operating conditions on de-NO_x performance. In our first report of numerical analysis, the influence of the pulse width and magnitude of the electric field of a single pulse on denitrification characteristics was examined,[1] and the influence of the gas composition, gas temperature, and pressure was examined in the second report,[2] and optimal values were indicated. Here we numerically analyze de-NO_x performance under repeated discharge of as many as 1000 pulses in an effort to have more realistic conditions. In the case of repetitive discharge, particularly in as many as 1000 pulses, the influence of accumulated by-products must be made clear. The amount of ammonia injected, which is known to improve de-NO_x performance, must also be optimized. Although we have obtained some understanding of the effects of additives and the influence of by-products through experimental research[3] and numerical analysis,[4,5] a better grasp of these factors is required. Here we aim to further clarify these factors by numerically analyzing the influence of by-products and the effect of an ammonia additive.

II. METHOD OF NUMERICAL ANALYSIS

A. Model

The pulse-discharge de-NO_x process can roughly be divided into two parts, one is the rapid electron collision pro-

cess where discharge electrons are accelerated and multiplied in a electric field and collide with combustion flue gas, such as H_2O and N_2, and produce OH and N radicals, and the other is the chemical reaction process where the radicals react with NO_x relatively slowly. In repetitive pulse discharges, the rapid electron collision process and the slow chemical reaction process proceed alternately. Further, they progress nonuniformly within an actual discharge reactor. Since the electric field is spatially distributed, the discharge de-NO_x process progresses nonuniformly. When performing analysis with this spatial distribution in mind, the calculation time and computer capacity increase. Therefore in our analysis, the flue gas is assumed to flow uniformly without any distribution in the reactor, and is uniformly exposed to square-wave pulses with the electron collision and chemical reaction processes proceeding with spatial uniformity.

The electron collision process is described by a kinetic equation using the reaction rate constant k_e. The rate constant k_e is described by the energy distribution function of electrons determined by the Boltzmann equation and the electron collision cross section. However, the calculation time and computer capacity to numerically analyze the Boltzmann equation are enormous in repetitive pulse discharge, like in this study. The constant k_e can be simply determined as follows if it is assumed to be dependent only on the reduced electric field. In this study, constant k_e dependent on the reduced electric field was determined by separate calculation of the Boltzmann equation changing parametrically the reduced electric field under a typical gas composition. Since the gas composition changes only a little during the discharge de-NO_x process discussed in this study, constant k_e can be well approximated to be dependent simply on the reduced electric field.[5] The rate constants k_e obtained in such a manner are listed in the Appendix.

Using this rate constant k_e, the electron collision process is calculated to get the concentration of unstable chemical species, and calculate the chemical reaction process between unstable and stable chemical species. The change in concentration of 101 chemical species following the repetitive pulse sequence was calculated by taking into account the 1004 rate equations for the electron collision and chemical reaction processes. The collision cross sections required for the rate constants of electron collision processes quoted are from Ref. 6. The rate constants quoted for the chemical reaction process are mainly from the National Institute for Standards and Technology (NIST) database,[7] and work by Matzing,[8] and by Delcroix.[9]

B. Method of calculation

A semi-implicit method was adopted here for stable calculation of the change in time of each chemical species concentration using all 1004 rate equations. The magnitude of the time step Δt was also varied. The rate of change of each chemical species concentration per Δt was normally set below 0.1. Adoption of this variable time step allowed us to efficiently calculate two different rate equations, one the electron collision process that rapidly proceeds during application of the pulse, and the other is the chemical reaction process that proceeds relatively slowly between pulses. In comparing our calculated results to those by the calculation code of discharge chemistry "KINEMA,"[10] our change in concentration of main chemical species per pulse agrees well with that by KINEMA within 0.1% error.

C. Comparison of our calculation with actual experiment

Our calculation results were compared with reported experimental results to verify whether or not our calculation model and our data adopted here such as the electron collision cross section and reaction rate constants are suitable. Here we have not considered the existence of Ar in air. In a case where Ar is considered, Ar deactivates the excited state of the O atom and reduces the efficiency of N_xO_y removal. But we have not considered Ar, because the difference in our calculated efficiency between the case with Ar and the case that ignores Ar is small.

Calculation conditions were put into the experimental conditions of methane combustion flue gas by Amirov *et al.*,[11] i.e.,

$$N_2:O_2:CO_2:H_2O:NO = 71:0.5:9.5:19:0.0165\%,$$

temperature of 290 K, pressure of 0.1013 MPa, pulse width of 100 ns, repetitive frequency of 1.1 kHz, and 14 300 repetitions. Attention must be paid to the electric field used in the calculation. The electrode configuration adopted in the compared experiment is coaxial cylinder type. Since the electric field in corona discharge is not uniform, we must be careful which electric field is selected in the nonuniform distribution as being representative. Similar to the common method in the field of discharge chemistry, the reduced electric field is set at 151 Td so as to match the experimental power consumption rate. When calculating under these conditions, the decrease in concentration due to denitrification is 66 ppm. The experimental decrease of 52 ppm shows good agreement with our calculation.

One more calculated example was compared with the experiment at a reactor of rectangular duct by Kato *et al.*[12] The calculation parameters matched the experimental conditions, i.e.,

$$N_2:O_2:CO_2:H_2O:NO:NH_3 = 70.5:1.8:9.9:17.9:0.031:0.031\%,$$

temperature of 373 K, pressure of 0.1013 MPa, pulse width of 100 ns, repetitive frequency of 180 Hz, 2300 repetitions, and reduced electric field of 161 Td. The calculated decrease in concentration was 260 ppm, while the experimental decrease was 150 ppm. The amount of NO_x decrease was somewhat larger in the calculation.

Although there is some discrepancy in the above two examples, our model can approximately predict the experimental results, and is considered appropriate although our calculation model and our data adopted here are limited.

D. Calculation conditions

Assuming combustion flue gas from an oil-fired power plant, the initial gas condition is set at

$$N_2:O_2:CO_2:H_2O:NO=72:1:15:12:0.03\%,^{13}$$

temperature $T=373\,\mathrm{K}$, and pressure $P=0.1013\,\mathrm{MPa}$. The initial electron density is assumed to be 10^9 particles/m^3, for which small electron density can be produced in the atmosphere by cosmic rays.[14]

The reduced electric field is set at 180 Td (corresponding to an electric field of 35 kV/cm) and the pulse width at 22 ns. This pulse width is shorter by one order than the value attainable by current pulse power technology. On the other hand, we aimed in this study for the electric power consumed for the discharge de-NO_x process be less than 5% of the power plant output,[15] i.e., the ratio of power consumed by the de-NO_x process to the total output from the power plant is less than 5%. Although the de-NO_x energy consumption rate with the reduced electric field and pulse width selected was calculated to be 48 eV/mol[1] and exceeded 5% when converted to the ratio of power consumed by the de-NO_x process, there is a possibility that it might be lower than 5% if ammonia is injected. Furthermore, if the ratio is less than 5%, the discharge de-NO_x process might be competitive with other de-NO_x processes such as the electron-beam process. Based on these estimates, the pulse width was set at 22 ns as a target for future technology.

The number N of repetitive pulses was set at 1000. If the reduced electric field and the pulse width are set at 180 Td and 22 ns, respectively, our previous study[1] shows that the NO_x removal efficiency becomes 0.15%, and if the same NO_x removal efficiency is maintained for each pulse, the total removal efficiency for 1000 pulses can be expressed by $[1-(1-\eta_i^{\mathrm{rem}}/100)^N]=0.78$. In this study, N is assumed to be roughly 1000 for attaining removal efficiency of nearly 80%. The repetitive frequency adopted in this study is set at 100 Hz, which is the typical frequency reported in many experimental studies.

The amount of ammonia injected was varied as a parameter from 0 to 600 ppm. The injection of ammonia promotes the NO_x removal process by oxidation as follows:

$$\mathrm{NO} \xrightarrow{\mathrm{O}} \mathrm{NO_2} \xrightarrow{\mathrm{OH}} \mathrm{HNO_3} \xrightarrow{\mathrm{NH_3}} \mathrm{NH_4NO_3}. \quad (1)$$

The nitrogen oxide formed in the above equation is neutralized and removed by the ammonia injected. According to Eq. (1), ammonia should be added in stoichiometric amounts of the initial NO concentration, but part of NO_x is also reduced and removed by N radicals and NH_2 radicals generated by NH_3. Therefore an amount of ammonia additive, which is smaller than the ammonia concentration but stoichiometrically equivalent to the initial NO concentration, is estimated to be an optimal value. To avoid complexity when ammonia was added, the sum of the initial gas composition rate was set at 100% by reducing the amount N_2 concentration supplied.

Under these conditions, assuming the gas temperature and pressure are constant, the repetitive pulse discharge process was numerically calculated. When flue gas is repeatedly exposed to the discharge pulse, the gas temperature rises by joule heating. However, the rise in temperature is calculated to be only a few tens of degrees, small enough that the rise in temperature produces little change in the de-NO_x process, only the numerical results under constant gas temperature are used hereafter.

E. Evaluation indicators of de-NO_x performance

The influence of by-products and the effect of injected ammonia are evaluated according to the NO_x removal efficiency and de-NO_x energy consumption rate defined below. In evaluating de-NO_x performance, it is necessary to consider not only the decrease in initial NO, but also the increase/decrease in total N_xO_y, such as the increase and accumulation of N_2O and so on, during repetitive discharges. In this article a total of 19 chemical species is accounted for as N_xO_y, i.e., NO, NO^+, NO^-, NO_2, NO_2^-, NO_2^+, NO_3, NO_3^-, N_2O, N_2O^+, N_2O_3, N_2O_4, N_2O_5, $NO^-(H_2O)$, $NO_2^-(H_2O)$, $NO^+(H_2O)$, $NO^+(H_2O)_2$, $NO^+(H_2O)_3$, and $NO_2^+(H_2O)_2$. Also HNO_2 might produce N_xO_y after HNO_2 is released into the atmosphere, because HNO_2 is photodissociated into NO and OH by illumination of light of short wavelength, less than 400 nm.[16] Considering this possibility we also calculated the NO_x removal efficiency and de-NO_x energy consumption rate including HNO_2 as N_xO_y.

The NO_x removal efficiency is defined as the increase/decrease rate in N_xO_y concentration based on the initial NO concentration. Since the removal efficiency changes with each pulse during repetitive pulses, the efficiency at the ith pulse is defined as follows:

$$\eta_i^{\mathrm{rem}}=\frac{[\mathrm{N_xO_y}]\ \text{at}\ (i-1)\text{th pulse}-[\mathrm{N_xO_y}]\ \text{at}\ (i)\text{th pulse}}{\text{initial}[\mathrm{NO}]}, \quad (2)$$

where [M] represents the concentration of chemical species M. The removal efficiency up to the Nth pulse is expressed by the following equation, using Eq. (2):

$$\eta_N^{\mathrm{rem}}=\sum_{i=1}^{\mathrm{N}}\eta_i^{\mathrm{rem}}. \quad (3)$$

The de-NO_x energy consumption rate is defined as the electrical energy required to remove one molecule of N_xO_y. Using the energy Q_i consumed at the ith pulse, the de-NO_x energy consumption rate for the ith pulse is defined as follows:

$$\eta_i^{\mathrm{cons}}=\frac{Q_i}{\text{initial}[\mathrm{NO}]\times\eta_i^{\mathrm{rem}}}. \quad (4)$$

The de-NO_x energy consumption rate up to the Nth pulse is defined as follows:

$$\eta_N^{\mathrm{cons}}=\frac{\Sigma_{i=1}^{N}Q_i}{\text{initial}[\mathrm{NO}]\times\eta_N^{\mathrm{rem}}}. \quad (5)$$

The value of Q_i can be obtained by integrating the product of the electron concentration, drift velocity, and electric field during the pulse width. The electron drift velocity was approximated as a function of the reduced electric field by solving the Boltzmann equation beforehand similar to the reaction rate constant for the electron collision process described in Sec. II A.

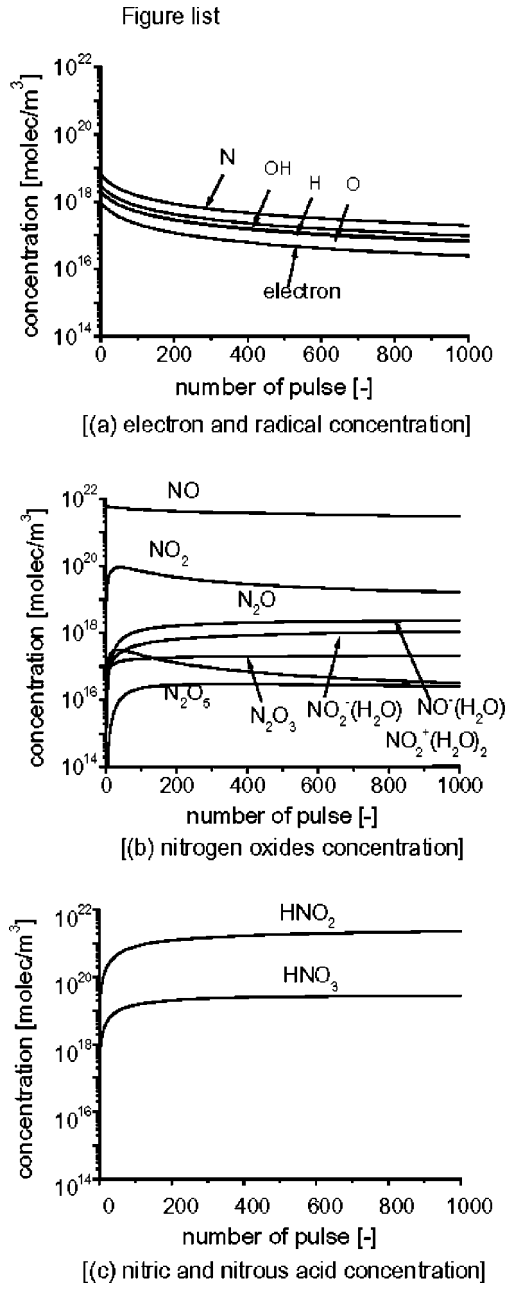

FIG. 1. Change in concentration of important chemical species with repetitive pulses without ammonia injection.

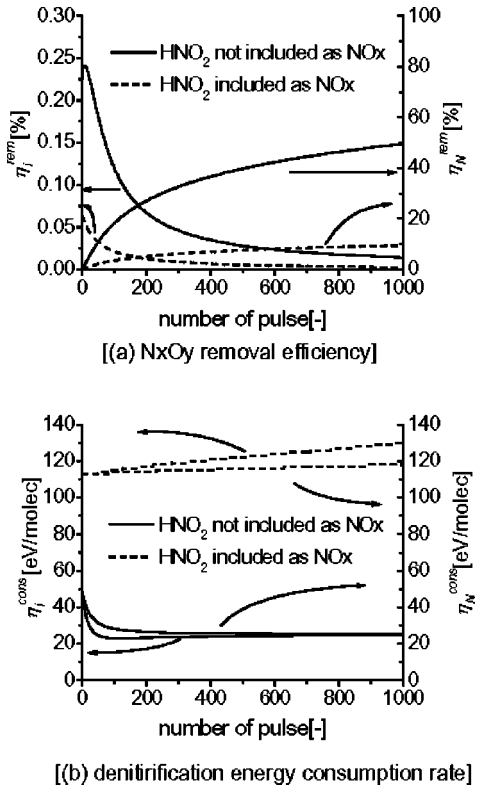

FIG. 2. Denitrification without ammonia injection.

III. CALCULATED RESULTS AND DISCUSSION

A. Results without ammonia injection

The concentration changes of the main chemical species without ammonia injection are shown in Fig. 1. Since it is complicated to show the concentration changing with each pulse, the concentration immediately after the end of each pulse only is plotted. Electrons and radicals such as N and OH are generated with each pulse. NO is oxidized and removed as shown in the following equations:

$$\mathrm{NO} \xrightarrow{\mathrm{O}} \mathrm{NO_2} \xrightarrow{\mathrm{OH}} \mathrm{HNO_3}, \tag{6}$$

$$\mathrm{NO} \xrightarrow{\mathrm{OH}} \mathrm{HNO_2}, \tag{7}$$

by the radicals generated, and gradually decreases. However, nitrogen oxides such as NO_2 and N_2O accumulate as by-products. Although it is not clearly shown in Fig. 1, NO is also removed by a reduction process as it reacts with the N radical and produces N_2.[1]

De-NO_x performance when ammonia is not injected is evaluated using the removal efficiency and the de-NO_x energy consumption rate defined in Sec. II E. In the case where HNO_2 is not considered N_xO_y, the removal efficiency for each pulse decreases from 0.24% to 0.01% when the pulse number increases as shown by the solid line in Fig. 2(a). This decrease is due to the decrease in electron and radicals concentration of Fig. 1(a) as the pulse number increases, which reduces the amount of NO removed by oxidation/reduction reactions. A total of 1000 pulses gives removal efficiency of 49%.

In the case where HNO_2 is not considered as N_xO_y, the de-NO_x energy consumption rate η_i^{cons} for each pulse rapidly decreases at the start of the pulse, as shown by the solid line in Fig. 2(b). Thereafter, it becomes constant at 25 eV/mol. Since the electron concentration, electric current, energy consumption rate Q_i, and removal efficiency decrease with an increase in pulse number, η_i^{cons} becomes constant through its definition, Eq. (4). Over 1000 pulses, η_i^{cons} also becomes approximately 25 eV/mol. Meanwhile in the case where HNO_2 is considered N_xO_y, the NO_x removal efficiency decreases and the de-NO_x energy consumption rate increases as shown by the dotted lines in Fig. 2, because half of N_xO_y is HNO_2. Therefore HNO_2 should be removed, i.e., neutralized by alkaline material such as NH_3.

Since the electron concentration decreases with each

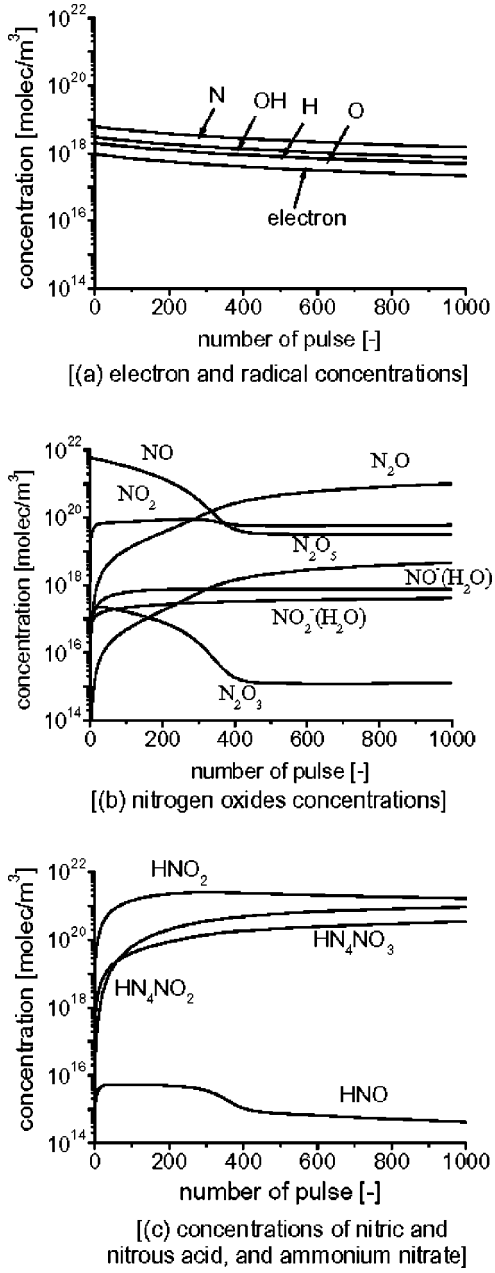

FIG. 3. Change in concentration of main chemical species with repetitive pulses with ammonia injection.

pulse in a repetitive pulse discharge, it is clear that the de-NO_x process does not proceed identically for each pulse. The reason why the electron concentration decreases as the pulse number increases is the increase in reaction rate for electron–ion recombination, shown by

$$e + H_3O^+(H_2O)_2 \rightarrow 3H_2O + H. \tag{8}$$

That is, when the pulse number increases, a long-lived by-product like $H_3O^+(H_2O)_2$ accumulates, and the recombination rate increases and results in a decrease in electron concentration.

B. Results with ammonia injection

The change in the main chemical species is shown in Fig. 3 when the repetitive pulse frequency is 100 Hz and 300 ppm of ammonia is added. The NO concentration rapidly decreases when ammonia is added. This is due to the removal of oxidation of NO promoted by the reactions of Eqs. (1), (9) and (10),

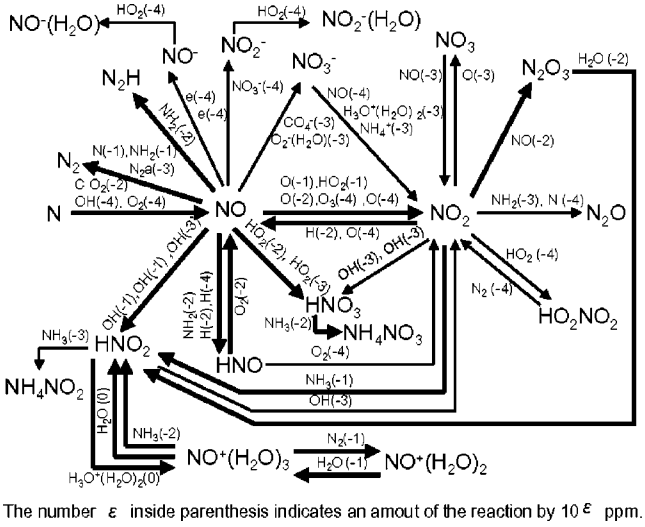

FIG. 4. Main reaction paths for removing NO and NO_2 between the 10th and 11th pulse.

$$NO \xrightarrow{OH} HNO_2 \xrightarrow{NH_3} NH_4NO_2, \tag{9}$$

$$NO_2 \xrightarrow{NH_3} HNO_2 \xrightarrow{NH_3} NH_4NO_2. \tag{10}$$

But in the case where HNO_2 is included in N_xO_y, the removal efficiency increases only slowly even when NH_3 of 300 ppm stoichiometrically equivalent to NO is injected, because there is so much HNO_2.

When ammonia is added, the electron concentration decreases with an increase in pulse number similar to the way when ammonia is not added. This is due to the accumulation of NH_4^+ in addition to $H_3O^+(H_2O)_2$, mentioned in Sec. III A, to neutralize electrons.

When the main reaction paths are illustrated, like in Fig. 4, it is clear that reduction removal of NO is also promoted by ammonia. NO is reduced to N_2 by the NH_2 radicals produced in dissociation of ammonia that has collided with discharge electrons,

$$NO \xrightarrow{NH_2} N_2. \tag{11}$$

Figure 4 is a diagram of the main path and shows chemical species with comparatively large reaction quantities with regard to NO and NO_2, which is obtained by integrating all of the reaction rate equations from the 10th pulse to the 11th pulse.

Calculated results with different amounts of ammonia additive ranging from 0 to 600 ppm are shown in Fig. 5 by the removal efficiency of Eq. (3) and by the energy consumption rate of Eq. (5) to the *N*th pulse. In Fig. 5 the case where HNO_2 is not considered N_xO_y is shown by the solid line, and the case where HNO_2 is considered N_xO_y is shown by the dotted line. The addition of ammonia increases the

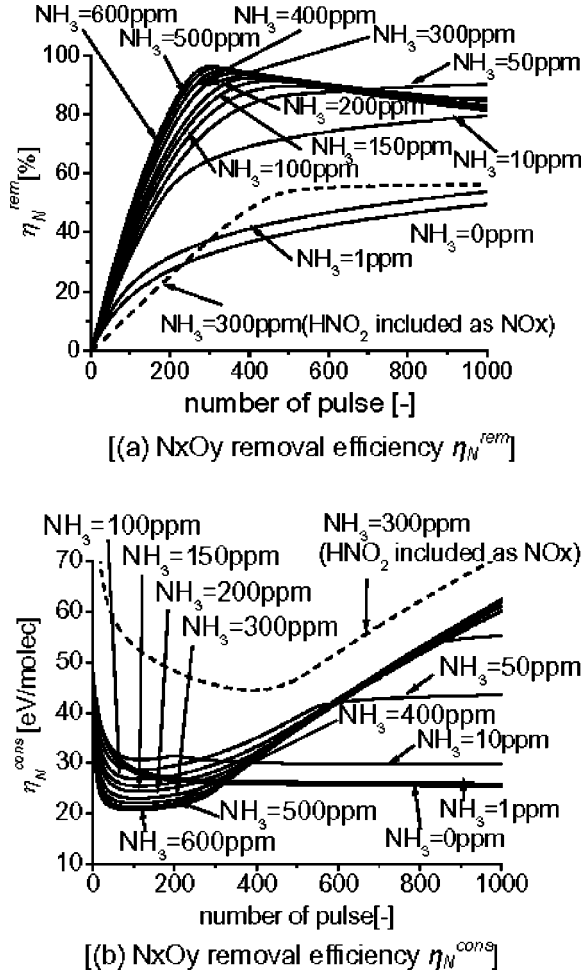

FIG. 5. Change in denitrification according to pulse number with ammonia injection.

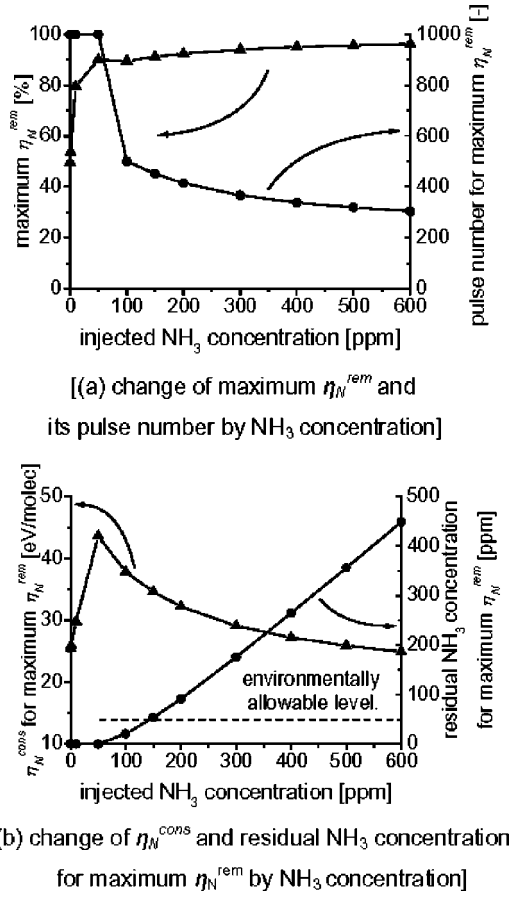

FIG. 6. Change of maximum η_N^{rem}, η_N^{cons}, and residual NH_3 concentration according to the injected NH_3 concentration.

NO_x removal efficiency. When 10 ppm of ammonia is injected, the de-NO_x efficiency is double the efficiency without ammonia injection. Maximum efficiency is observed when 100 ppm or more of ammonia is added. N_xO_y decreases at the pulse number prior to maximum efficiency, but N_xO_y increases at the pulse number after the maximum. The maximum efficiency in the vicinity of 100 ppm ammonia is reflected in the minimum de-NO_x energy consumption rate. For a total of 1000 pulses, the energy consumption rate for the case with ammonia addition becomes larger than that with no ammonia addition.

The maximum removal efficiency and the minimum de-NO_x energy consumption rate originate from the conversion of NO_2 to N_2O, as shown in Figs. 3(b) and 4. When flue gas is exposed to repetitively pulsed discharge, the O radical oxidizes NO and forms NO_2. If an additional amount of ammonia is suitable, NO_2 is removed by Eqs. (1) and (10). However, when ammonia is added in excess, NO_2 is converted into N_2O, which is a greenhouse gas, by the large amount of NH_2 radical generated in the pulsed discharge,

$$NO_2 \xrightarrow{NH_2} N_2O. \tag{12}$$

The conversion to N_2O by Eq. (12) and the generation of a small amount of NO and NO_2 during discharge result in maximum removal efficiency through its definition, Eq. (2) or (3).

C. Optimal amount of ammonia added and pulse number

When the amount of ammonia added is changed, the removal efficiency shows a maximum value, and the de-NO_x energy consumption rate shows a minimum value, as was shown in Sec. III A, when the pulse number increases. It is also clear that the pulse number for the maximum or the minimum depends on the amount of ammonia added. This means that an optimal amount of ammonia added and pulse number exist for the pulsed discharge de-NO_x process.

Figure 6(a) shows the maximum removal efficiency and the pulse number for maximum efficiency when the amount of ammonia added is changed. Since an ammonia concentration of less than 50 ppm does not give maximum removal efficiency, the plots in Fig. 6 are for the 1000th pulse. Figure 6(b) shows the de-NO_x energy consumption rate that corresponds to maximum removal efficiency. In order to attain high de-NO_x performance, it is clear from Figs. 6(a) and 6(b) that high removal efficiency of more than 90% and a de-NO_x energy consumption rate less than 30 eV/mol are attainable when more than 300 ppm of ammonia is injected and approximately 300 pulses are applied. However, at the end of a

discharge process of about 300 pulses with a large amount of ammonia added, a large quantity of residual ammonia still remains. The ammonia concentrations shown in Fig. 6(b) remains at the end of a discharge process when the pulsed discharge is stopped at the pulse number for maximum removal efficiency. When a suitable discharge de-NO_x device is adopted in an automobile or a distributed power source, the upper limit of the ammonia exhaust concentration seems to be about the same as the permissible concentration of 50 ppm[17] for residences and the workplace. However, Fig. 6(b) shows that the residual ammonia concentration exceeds this value.

From the standpoint of both permissible ammonia concentration and high de-NO_x performance, suitable operating conditions are to inject 150 ppm of ammonia and to apply approximately 450 repeated pulses. Under these conditions, high performance with a removal efficiency of about 90% and de-NO_x energy consumption rate of approximately 35 eV/mol are obtained. Although the above discussion was induced from the maximum removal efficiency in Fig. 5(a), similar results can be obtained from the minimum energy consumption rate in Fig. 5(b). For simplicity, the discussion here was summarized only by the maximum removal efficiency.

D. Practical possibilities

The practical possibilities for this repetitively pulsed discharge method were compared here to other de-NO_x methods in terms of efficiency and size. As described earlier, the performance of a repetitively pulsed discharge device differs depending on its operating conditions. In the present study, the discharge device is compared to other devices when the former is operated at 150 ppm of ammonia and 450 repeated pulses, which is equivalent to removal efficiency η_N^{rem} of 90% and energy consumption rate η_N^{cons} of 34.6 eV/mol. A discharge de-NO_x device with this performance could be used in a fossil-fuel-fired power plant with electrical output E_{power} of 1680 kW, flue gas flow rate $\dot{V}$ of 14 400 m^3 N/h, and initial NO concentration [NO] of 300 ppm.[1] The number of molecules of processed nitrogen oxide $\dot{\mathrm{M}}_{\mathrm{N_xO_y}}$ per second is determined by the equation below using the de-NO_x rate,

$$\dot{\mathrm{M}}_{\mathrm{N_xO_y}} = \frac{\dot{V}}{RT} P \frac{[\mathrm{NO}]}{10^6} \eta_N^{\mathrm{rem}} N_A = 0.21 \times 10^{23} \ \ \mathrm{mol/s}, \qquad (13)$$

where R represents the gas constant, T and P represent gas temperature of 373 K and pressure of 0.101 MPa, described in Sec. II D, and N_A represents the Avogadro number. The electric energy $E_{\text{de-NO}_x}$ required for denitrification is given by,

$$E_{\text{de-NO}_x} = \dot{\mathrm{M}}_{\mathrm{N_xO_y}} \eta_N^{\mathrm{cons}} = 117.6 \ \ \mathrm{kW}. \qquad (14)$$

Accordingly, the de-NO_x device consumes 7% of electrical output from the power plant, i.e., $E_{\text{de-NO}_x}/E_{\mathrm{power}} = 7\%$. Since electron beam de-NO_x devices consume about 3% of electrical output from the power plant,[1] the de-NO_x performance of a repetitively pulsed discharge device is rather low. However, because the constitution of the discharge de-NO_x device is relatively simple compared to the electron beam device, the discharge device seems to be competitive with the electron beam device due to the low cost of construction of the simple discharge device.

The size of the pulsed discharge de-NO_x device is determined mainly by that of the discharge reactor, described as follows. When we let combustion flue gas flow slowly at a velocity of about 1 m/s so as to be excited by repetitive pulses, the reactor cross section orthogonal to the flow direction is calculated to be 4 m^2. The reactor length becomes 1 (m/s)$\times$0.01 (s)$\times$450 [$-$]=4.5 (m) under gas velocity of 1 m/s, repetition frequency of 100 Hz (period of 0.01 s), and 450 repeated pulses. Considering the total site of a fossil-fuel-fired power plant, a discharge reactor that occupies only about 4 $\mathrm{m}^2 \times 4.5$ m might be small enough to be permissible for the plant.

When applied to a compact diesel engine of the several kW class, a severe de-NO_x energy consumption rate of about 10 eV/mol is required because efficiency is reduced in a smaller engine.[15] Since the consumption rate in the present study is about 35 eV/mol, it would be difficult to apply the pulsed discharge de-NO_x device to small diesel engines. However, because some reports indicate a twofold performance improvement when a hydrocarbon such as propylene,[15,18] which is not considered in the present study, is injected, we would like to investigate the improvement of the pulsed discharge de-NO_x process using hydrocarbon injection.

IV. CONCLUSION

The performance of a repetitive pulse discharge de-NO_x process was numerically analyzed by considering a total of 1004 rate equations of combined electron collision and chemical reaction processes. Under representative conditions with reduced electric field of 180 Td, pulse width of 22 ns, pulse repetition frequency of 100 Hz, and 1000, repetitions the de-NO_x performance was calculated by parametrically changing the amount of ammonia injected and the results are the following.

(1) When ammonia is not injected, NO_x is removed by oxidation reactions with O and OH radicals and by a reduction reaction with the N radical. However, the de-NO_x performance gradually degrades with each pulse repetition because the discharge electrons recombine with accumulated water cluster ions and decrease the electron density.
(2) When ammonia is injected, ammonium nitrate forms through the reaction of ammonia and nitric acid, and promotes the oxidation removal process. The NO reduction removal process is also promoted by the NH_2 radical, which forms through electron collision dissociation of ammonia. Both of these effects by ammonia injection improve de-NO_x performance.
(3) When ammonia is injected in excess, the NO_x removal efficiency shows a maximum and the de-NO_x energy consumption rate shows a minimum relative to the repetitive pulse number. When an environmentally permissible ammonia concentration is considered, there is an

appropriate amount of ammonia injected as well as a number of repetitive pulses, 150 ppm, and 450 pulses, respectively, under the conditions in the present study. At these settings, the NO_x removal efficiency is 90% and the de-NO_x energy consumption rate is 35 eV/mol.

(4) When the pulsed discharge de-NO_x device with the above performance is adopted in a fossil-fuel-fired power plant, the ratio of power consumed at the de-NO_x device to the power generated at the power plant is calculated to be 7%. Considering the simplicity of the device, the discharge de-NO_x process may be competitive with the electron beam de-NO_x process.

(5) When HNO_2 is considered N_xO_y due to its photodissociation to NO in the atmosphere, the de-NO_x performance is somewhat reduced because the HNO_2 produced remains in the pulsed discharge process.

ACKNOWLEDGMENTS

The authors express their sincere thanks to lecturer Kuniyasu Ogawa, School of Engineering, Keio University, for his guidance in designing the numerical model, and to the Steel Industry Foundation for the Advancement of Environmental Protection Technology and Toyohashi University of Technology for partial support of this study.

APPENDIX

Under the representative conditions shown in Sec. II D, the Bolztmann equation for the electron energy distribution was numerically calculated, and the reaction rate constants were determined from the electron energy distribution and the electron collision cross section obtained. The Boltzmann equation was numerically calculated parametrically by changing the reduced electric field, and the rate constants by the electron collision process were adjusted as a function of the reduced electric field. The list below shows reaction rate constants k (cm^6/s) and k^* (cm^9/s) at representative reduced electric fields of 180 Td for the present calculations.

(1) $N_2+e\rightarrow N_{2r}+e, \quad k=6.68\times10^{-9}$,

(2) $N_2+e\rightarrow N_{2v1}+e, \quad k=3.78\times10^{-9}$,

(3) $N_2+e\rightarrow N_{2A}+e, \quad k=3.37\times10^{-10}$,

(4) $N_2+e\rightarrow N_{2a}+e, \quad k=2.85\times10^{-10}$,

(5) $N_2+e\rightarrow N_2^++e, \quad k=4.48\times10^{-11}$,

(6) $N_2+e\rightarrow N+N+e, \quad k=2.11\times10^{-10}$,

(7) $N+e\rightarrow N^++2e, \quad k=1.10\times10^{-10}$,

(8) $N_{2a}+e\rightarrow N_2^++2e, \quad k=1.74\times10^{-9}$,

(9) $N_{2a}+e\rightarrow N_2^++2e, \quad k=4.28\times10^{-10}$,

(10) $O_2+e\rightarrow O_{2r}+e, \quad k=1.66\times10^{-11}$,

(11) $O_2+e\rightarrow O_{2v1}+e, \quad k=6.95\times10^{-11}$,

(12) $O_2+e\rightarrow O_2^++2e, \quad k=1.32\times10^{-10}$,

(13) $O_2+e\rightarrow O_{2a1D}+e, \quad k=6.81\times10^{-10}$,

(14) $O_2+e\rightarrow O_{2B1S}+e, \quad k=1.58\times10^{-10}$,

(15) $O_2+e\rightarrow O+O+e, \quad k=4.81\times10^{-9}$,

(16) $O_2+e\rightarrow O^-+O, \quad k=3.79\times10^{-11}$,

(17) $O_2+e+M\rightarrow O_2^-+M, \quad k^*=6.30\times10^{-36}$,

(18) $O+e\rightarrow O^++2e, \quad k=1.06\times10^{-10}$,

(19) $O+e\rightarrow O_{1D}+e, \quad k=2.13\times10^{-9}$,

(20) $O+e\rightarrow O_{1S}+e, \quad k=1.45\times10^{-10}$,

(21) $O_{2a1D}+e\rightarrow O+O+e, \quad k=1.01\times10^{-9}$,

(22) $O_{2a1D}+e\rightarrow O_2^++2e, \quad k=4.14\times10^{-10}$,

(23) $O_{2B1S}+e\rightarrow O+O+e, \quad k=1.01\times10^{-9}$,

(24) $O_{2B1S}+e\rightarrow O_2^++2e, \quad k=4.56\times10^{-10}$,

(25) $N_2O+e\rightarrow N_2+O^-, \quad k=1.43\times10^{-10}$,

(26) $O_3+e\rightarrow O_3^++2e, \quad k=2.34\times10^{-11}$,

(27) $H_2O+e\rightarrow H_2O_{v1}+e, \quad k=5.26\times10^{-9}$,

(28) $H_2O+e\rightarrow H+OH+e, \quad k=6.55\times10^{-10}$,

(29) $H_2O+e\rightarrow O_{1D}+H_2+e, \quad k=3.32\times10^{-11}$,

(30) $H_2O+e\rightarrow H_2O^++2e, \quad k=5.05\times10^{-11}$,

(31) $H_2O+e\rightarrow OH^-+H, \quad k=3.38\times10^{-12}$,

(32) $H_2O+e\rightarrow H^-+OH, \quad k=9.18\times10^{-11}$,

(33) $H_2O+e\rightarrow H_2+O^-, \quad k=1.33\times10^{-11}$,

(34) $CO_2+e\rightarrow CO_{2v1}+e, \quad k=7.36\times10^{-9}$,

(35) $CO_2+e\rightarrow CO_2^++2e, \quad k=1.41\times10^{-10}$,

(36) $CO_2+e\rightarrow CO+O^-, \quad k=6.04\times10^{-12}$.

[1] K. Ito, K. Hagiwara, H. Nakamura, K. Onda, and H. Tanaka, Electr. Eng. Jpn. **139**, 1 (2002).
[2] K. Ito, K. Hagiwara, H. Nakamura, K. Onda, and H. Tanaka, Trans. Inst. Electr. Eng. Jpn., Part B **122**, 216 (2002).
[3] T. Namihira, H. Hori, D. Wang, S. Tsukamoto, S. Katsuki, H. Akiyama, M. Shimizu, and K. Yokohama, Trans. Inst. Electr. Eng. Jpn., Part A **121**, 834 (2001).
[4] A. C. Gentile and M. J. Kushner, J. Appl. Phys. **78**, 2074 (1995).
[5] J. J. Lowke and R. Morrow, IEEE Trans. Plasma Sci. **23**, 661 (1995).
[6] JILA Information Center Report Nos. 13, 26, and 28, University Colorado, Boulder, CO (1985)
[7] F. Westley, D. H. Frizzell, J. T. Herron, R. F. Hampson, and W. G. Mallard, NIST Chemical Kinetics Database Ver. 6.01, U.S. Dept. Commerce, Gaithersburg, MD (1994).
[8] H. Matzing, Adv. Chem. Phys. **80**, 315 (1991).
[9] J. I. Delcroix, *Gas Phase Chemical Physics Database* (Elsevier, New York, 1987).
[10] http://www.kinema.com (2003).
[11] R. H. Amirov, E. I. Asinovsky, I. S. Samoilov, and A. V. Shepelin, Plasma Sources Sci. Technol. **2**, 289 (1993).
[12] K. Kato, K. Kasuga, M. Fujiwara, and K. Onda, Electr. Eng. Jpn. **116**, 94 (1996).
[13] I. Gallimberti, Pure Appl. Chem. **60**, 663 (1988).
[14] J. M. Meek and J. D. Craggs, *Electrical Breakdown of Gases* (Wiley,

New York, 1978), p. 655.
[15] Y. Yoshioka, Trans. Inst. Electr. Eng. Jpn., Part A **122**, 676 (2002).
[16] B. J. Finlayson-Pitts and J. N. Pitts, Jr., *Chemistry of The Upper and Lower Atmosphere Theory, Experiments and Applications* (Academic Press, New York, 2000), p. 99.
[17] H. Naito and N. Yokote, *Kagaku Bussitu Dokusei Handobukku* (Maruzen, Tokyo, 1999), Vol. 1, p. 328 (in Japanese).
[18] Y. S. Mok and I. Nam, IEEE Trans. Plasma Sci. **27**, 1188 (1999).